

AN INTERACTIVE BOUNDARY-LAYER METHOD FOR AIRFOILS

Horia DUMITRESCU, Vladimir CARDO^a

“Caius Iacob” Institute of Applied Mathematics, P.O.Box 1-24, RO-70700, Bucharest

Corresponding author: Horia Dumitrescu, e-mail: horiad@ns.ima.ro

A calculation method for the aerodynamic prediction of airfoils based on a new interactive boundary-layer approach and an improved Cebeci-Smith eddy viscosity formulation is described. Results are presented for airfoils at low and moderate Reynolds numbers in order to demonstrate the need to calculate transition for accurate drag polar and maximum lift coefficient prediction.

1. INTRODUCTION

In the last thirty years, there have been significant accomplishments in computational fluid dynamics (CFD). Whereas in the early 1960's panel methods and boundary-layer methods were being developed for relatively simple configurations, today the calculations are being performed routinely with Navier-Stokes methods not only simple configurations but also for complex aircraft configurations. The calculations performed with these methods lead to significant savings by reducing wind tunnel testing. Progress has been so impressive that one may even say that CFD has reached its maturity.

An area that still requires further work in CFD is the development of design methods for high lift configurations. The presence of high and low Reynolds number flows on various components of airfoils and significant regions of flow separation near stall conditions, as well as possible merging of shear layers, make the development of such a capability a challenging task.

The required generality and accuracy of the method and, equally important, its efficiency as a design tool, introduce additional challenges.

The current development of design algorithm for high lift configurations follows two approaches.

One approach is based on the solution of the Navier-Stokes equations with structured and unstructured grids [1-3]. The second approach is the one based on the interactive boundary layer theory and will form the basis for our presentation. This approach involves interaction between inviscid and boundary-layer equations. For low speed flows, the inviscid flow is often computed by a panel method, with or without compressibility corrections, and the viscous flow is computed by an inverse boundary-layer method [4-5]. This approach, though not as general as the Navier-Stokes approach, provides a good compromise between the efficiency and accuracy required in a design process [6].

Regardless of which approach is used to develop a computational tool for high lift configurations, it is necessary to calculate the onset of transition in order to identify the effect of wind tunnel and flight Reynolds numbers. Individual components of multi-element airfoils at wind tunnel Reynolds numbers have relatively lower Reynolds numbers than the main airfoil. At chord Reynolds numbers less than 500,000, the components can have large separation bubbles, with the onset of transition occurring inside the separation bubble. As a result, the behavior of the flow can be significantly different from the behavior of the main airfoil at higher Reynolds numbers. Furthermore, the transition can influence the drag coefficient. For this reason determining the onset transition is crucial for predicting drag polars, which are of

Recommended by Lazăr DRAGO^a
Member of the Romanian Academy

major interest when designing high-lift systems for take-off and climb requirements [6].

The present method describes an interactive-boundary-layer approach to the calculation of high lift configurations in two-dimensional flows. Results for two airfoils at high and low Reynolds numbers are presented and discussed.

2. CALCULATION METHOD

2.1. Inviscid Method

The calculation method is formulated for compressible flows and has been applied to single airfoils at low and high Reynolds number. A full potential method [7] is used to compute the inviscid flow with viscous effects provided by a new direct boundary-layer method [8]. The inviscid flow field is computed using Jameson's multiple grid alternating direction technique. The potential flow equation is treated in the conservation form:

$$\frac{\partial}{\partial x}(\rho U) + \frac{\partial}{\partial y}(\rho V) = 0 \quad (1)$$

where $U = \Phi_x$, $V = \Phi_y$.

At the profile, the potential satisfies the Neumann boundary condition:

$$\frac{\partial \Phi}{\partial n} = 0. \quad (2)$$

The discrete approximation used is a rotated central difference scheme with an artificial viscosity, which is suitable for airfoil calculation without restriction on the speed at infinity. Time-dependent terms have been added to embed the steady-state equation in a convergent time-dependent process. The solution of the resulting set of nonlinear difference equations is done by the multiple grid method.

2.2. Direct Boundary Layer Method

The boundary-layer method is based on the solution of the modified boundary-layer equations [8], which are suitable for direct calculation without restriction on the separation. With the algebraic eddy viscosity ε_m and turbulent Prandtl number P_t concepts, the compressible boundary layer equations and their boundary conditions on the airfoil and in the wake for an adiabatic surface are:

- continuity:

$$\frac{\partial}{\partial x}(\rho u) + \frac{\partial}{\partial y}(\overline{\rho v}) = 0 \quad (3)$$

- x -momentum :

$$\rho u \frac{\partial u}{\partial x} + \overline{\rho v} \frac{\partial u}{\partial y} - \frac{\partial}{\partial y} \left[(\mu + \rho \varepsilon_m) \frac{\partial u}{\partial y} \right] = \rho_e U \frac{\partial U}{\partial x} + \rho_e V_{EIF} \frac{\partial U}{\partial y} - \frac{\partial}{\partial y} \left[(\mu_e + \rho_e \varepsilon_m) \frac{\partial U}{\partial y} \right] \quad (4)$$

- energy:

$$\rho u \frac{\partial H}{\partial x} + \overline{\rho v} \frac{\partial H}{\partial y} - \frac{\partial}{\partial y} \left[\left(k + c_p \rho \frac{\varepsilon_m}{P_t} \right) \frac{\partial T}{\partial y} + (\mu + \rho \varepsilon_m) u \frac{\partial u}{\partial y} \right] = \rho_e U \frac{\partial H_e}{\partial x} + \rho_e V_{EIF} \frac{\partial H_e}{\partial y} - \frac{\partial}{\partial y} \left[\left(k + c_p \rho_e \frac{\varepsilon_m}{P_t} \right) \frac{\partial T_e}{\partial y} + (\mu_e + \rho_e \varepsilon_m) U \frac{\partial U}{\partial y} \right] \quad (5)$$

- equivalent inviscid velocity:

$$V_{EIF}(x, y) = \frac{\rho_{ew}}{\rho_e} V_w(x) - \frac{1}{\rho_e} \int_0^y \frac{\partial(\rho_e U)}{\partial x} dy \quad (6)$$

- transpiration velocity :

$$V_w(x) = \frac{1}{\rho_{ew}} \frac{d}{dx} \int_0^{\delta} (\rho_e U - \rho u) dy \quad (7)$$

where T is the temperature, H is a near value of the total enthalpy given by:

$$H = c_p T + \frac{u^2}{2} \quad \text{for boundary layer} \quad (8)$$

$$H_e = c_p T_e + \frac{U^2}{2} \quad \text{for inviscid flow} \quad (9)$$

and:

$$\overline{\rho v} = \rho v + \overline{\rho'v'}, \quad \frac{\rho_e}{\rho} = \frac{T}{T_e}, \quad \frac{\mu}{\mu_e} = \left(\frac{T}{T_e} \right)^\omega \quad (10)$$

On the airfoil, the boundary conditions are:

$$\begin{aligned}
y = 0, \quad u = 0, \quad v = 0, \quad \frac{\partial H}{\partial y} = 0 \\
y \geq \delta, \quad u = U(x, y), \quad v = V_{EIF}(x, y), \\
H = H_e(x, y).
\end{aligned} \tag{11}$$

In the wake, where a dividing line at $y=0$ is required to separate the upper and lower parts of the inviscid flow, in the absence of normal pressure gradient, the boundary conditions at $y=0$ are:

$$\begin{aligned}
y = 0, \quad \frac{\partial u}{\partial y} = 0, \quad v = 0, \quad \frac{\partial H}{\partial y} = 0 \\
y \geq \delta_w, \quad u = U(x, y), \quad v = V_{EIF}(x, y), \\
H = H_e(x, y).
\end{aligned} \tag{12}$$

The solution of the inviscid flowfield supplies U , P , and H_e . The proper matching of the boundary-layer solution with the inviscid solution, in magnitude and slope, allows the direct calculation of the separated flow for a prescribed velocity field $U(x, y)$.

The turbulence model for ε_m and P_r is given by an improved version of the Cebeci and Smith algebraic eddy viscosity formulation [9]. According to this model, P_r is taken as constant equal to 0.9 and ε_m is given by separate expressions for the inner and outer regions of the boundary layer:

$$\varepsilon_m = \begin{cases} (\varepsilon_m)_i = \left[0.4y \left(1 - \exp \frac{-y}{A} \right) \right]^2 \left(\frac{\partial u}{\partial y} \right) \gamma_{tr}, & 0 \leq y \leq y_c \\ (\varepsilon_m)_o = \alpha \int_0^\infty (U - u) dy \gamma_{tr} \gamma, & y_c \leq y \leq \delta, \end{cases} \tag{13}$$

where:

$$\alpha = \frac{0.0168}{F^{1.5}}, \quad A = 26 \frac{v}{u_\tau} \left(\frac{\rho}{\rho_w} \right)^{1/2}, \quad u_\tau = \left(\frac{\tau}{\rho} \right)_{\max}^{1/2} \tag{14}$$

The parameter F is related to the ratio of the product of the turbulence energy by normal stresses to that by shear stress evaluated at the location where the shear stress is maximum. As discussed in [9], it is given by:

$$F = 1 - \beta \frac{\partial u / \partial x}{\partial u / \partial y} \tag{15}$$

where the parameter β is a function of $R_t = \tau_w / (-\rho u'v')_{\max}$, which, for $\tau_w \geq 0$, is represented by:

$$\beta = \begin{cases} \frac{6}{1 + 2R_t(2 - R_t)}, & R_t \leq 1.0 \\ \frac{1 + R_t}{R_t}, & R_t \geq 1.0 \end{cases} \tag{16}$$

For $\tau_w \leq 0$, R_t is set equal to zero.

The improved turbulence model uses an intermittence expression applicable for flows with favorable and adverse pressure gradients as well as zero pressure gradient flows. It is based on Fiedler and Head's correlation [10] and is given by:

$$\gamma = \frac{1}{2} \left[1 - \operatorname{erf} \frac{y - Y}{\sqrt{2}\sigma} \right] \tag{17}$$

where Y and σ are general intermittence parameters with Y denoting the value of y where $\tilde{\alpha} = 0.5$ and σ denoting the standard deviation.

The condition used to define y_c in Eq. (13) is the continuity of the eddy viscosity, so that ε_m is defined by $(\varepsilon_m)_i$ from the wall outward (inner region) until its value is equal to that given for the outer region by $(\varepsilon_m)_o$.

The expression γ_{tr} models the transition region and is given by:

$$\gamma_{tr} = 1 - \exp \left(-G(x - x_{tr}) \int_{x_{tr}}^x \frac{dx}{U_w} \right) \tag{18}$$

Here, x_{tr} denotes the onset of transition and G is defined by:

$$G = \frac{3}{C^2} \frac{U_w^3}{v^2} R_{x_{tr}}^{-1.34} \tag{19}$$

where C is 60 for attached flows and the transition Reynolds number is $R_{x_{tr}} = (U_w x / v)_{tr}$. In the low Reynolds number range from $R_c = 2 \times 10^5$ to 6×10^5 , the parameter C is given by:

$$C^2 = 213 (\lg R_{x_{tr}} - 4.7323) \tag{20}$$

The corresponding expressions for the eddy-viscosity formulation in the wake are:

$$\varepsilon_m = (\varepsilon_m)_w + [(\varepsilon_m)_{t.e.} - (\varepsilon_m)_w] \exp \frac{-(x - x_0)}{l_w \delta_{t.e.}} \quad (21)$$

where $\delta_{t.e.}$ is the boundary layer thickness at the trailing edge, $l_w = 20$, $(\varepsilon_m)_{t.e.}$ is the eddy viscosity at the trailing edge, and $(\varepsilon_m)_w$ is the eddy-viscosity in the far wake given by the larger of:

$$(\varepsilon_m)_w^l = 0.064 \int_{-\infty}^{y_{\min}} (U - u) dy \quad (22a)$$

$$(\varepsilon_m)_w^u = 0.064 \int_{y_{\min}}^{\infty} (U - u) dy \quad (22b)$$

with y_{\min} denoting the location where the velocity is minimum.

2.3. Solution Procedure

The above equations are first expressed in transformed coordinates by means of the Falkner-Skan transformation. Using Keller's two-point finite difference method as described in [9] then numerically solves the transformed equations. Once a solution is obtained for the external velocity field given by the full potential method, the transpiration velocity distribution on the surface is calculated from Eq. (7) and a jump ΔV_w in the component of velocity normal to the airfoil dividing streamline:

$$\Delta V_w = V_w^u + V_w^l \quad (23)$$

is computed from the boundary-layer solutions. In the above equation superscripts u and l denote upper and lower sides of the dividing streamline.

The boundary conditions given by Eqs. (7) and (23) are then used in the potential method to replace the zero transpiration velocity at the surface and the calculated displacement thickness at the airfoil trailing edge is used to satisfy the Kutta condition. This procedure of computing inviscid and viscous flows is continued until the convergence of the solutions. It matches exactly all of the flow properties even when the inviscid flow has significant normal gradients.

3. RESULTS AND DISCUSSIONS

Figure 1 presents a comparison between measured [11] and computed lift and drag coefficients for the NACA0012 airfoil at a high chord Reynolds number of 3×10^6 . If the flow is attached, the onset of transition is determined by Michel's criterion and at high angles of attack, when the flow separates downstream of the pressure peak before the Michel's criterion can be satisfied, the onset of transition is chosen to coincide with laminar separation. To demonstrate the importance of computing transition as part of the method, calculations were also performed with transition fixed near the stagnation point for all angles of attack (dotted line). As can be seen, the results with computed transition show a much better agreement with experimental data than those in which the transition were fixed.

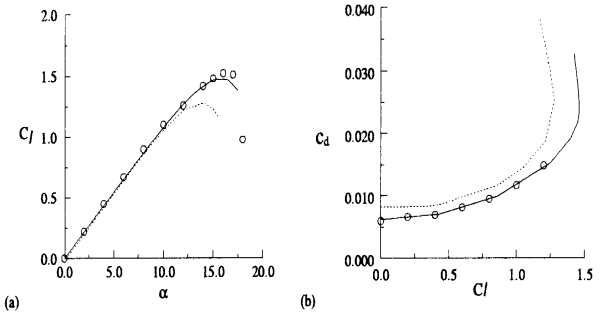


Fig. 1.-Lift (a) and drag (b) coefficients for NACA0012 airfoil.

The behavior of airfoils at low Reynolds numbers differs from that at high Reynolds numbers, in that rather large separation bubbles can occur downstream of the leading edge with transition taking place within the bubble prior to reattachment. The length of the bubble increases with decreasing Reynolds numbers and strongly influences the performance characteristics of the airfoil. For this reason, at low Reynolds numbers it is not possible to calculate the onset of transition with the Michel's criterion. Now, at low to moderate angles of attack, the onset of transition is calculated with the e^n - method and at higher angles of attack, where large separation is present, the onset of transition is assumed to correspond to the location of laminar flow separation.

Results are first presented for the ONERA-D airfoils tested by Cousteix and Pailhas [12] in a wind tunnel with a chord Reynolds number of 3×10^5 at zero angle of attack. The tested airfoil, mean velocity profiles and distributions of external

velocity and skin-friction coefficient are shown in Fig. 2. Measured and calculated results are in close agreement with larger differences only in the velocity profiles immediately upstream of boundary-layer separation ($x/c = 0.712$) where we may expect cross-stream pressure gradients and normal stresses to have a locally-important role. In this case, transition occurred within the separated flow region and caused reattachment shortly thereafter. The calculations revealed transition at $x/c = 0.79$ for $n = 8$, at $x/c = 0.81$ for $n = 9$ in the e^n - method, in comparison with measurements which revealed transition at $x/c = 0.808$.

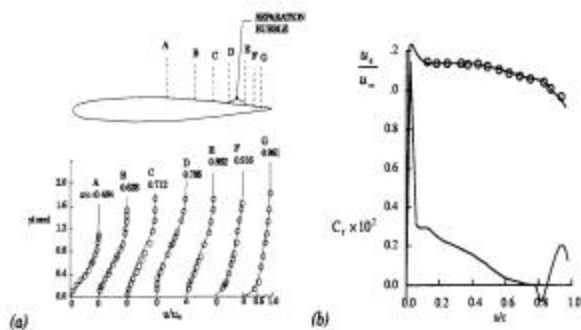


Fig. 2.- Velocity profiles (a) and external velocity and skin friction coefficient distributions (b).

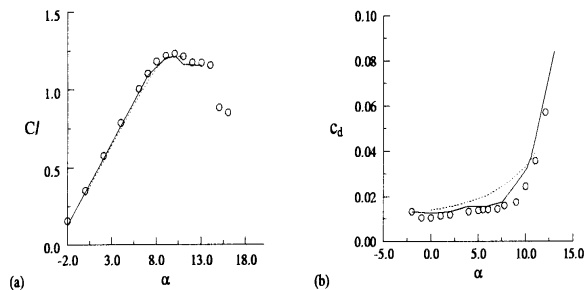


Fig. 3.- Lift (a) and drag (b) coefficients for Eppler airfoil.

Figure 3 shows the results for the Eppler 387 airfoil at a chord Reynolds number of 2×10^5 . Here, the location of transition does not play an important role in predicting lift coefficient. However, the calculations with the fixed transition location can be performed until $\alpha = 13.5^\circ$. As before, the drag coefficients obtained with the transition location computed show better agreement with data than those with a fixed transition location (dotted line).

4. CONCLUSIONS

An interactive boundary-layer method based on

new boundary-layer equations and an improved Cebeci-Smith eddy viscosity formulation is used to calculate the aerodynamic performance characteristics of airfoils at high angles of attack. In general, the predictions are excellent for relatively low angles of attack and very satisfactory up to stall. The study shows that the onset of transition location plays a significant role in predicting drag and that its calculation must be a part of the computational method. The study also shows the importance of the turbulence model in predicting maximum lift coefficient.

REFERENCES

1. ROGERS, S.E., WILTBERGER, N.L. KWAK, D., *Efficient simulation of incompressible viscous flow over single and multielement airfoils*, AIAA Paper, **92-0405**, 1992.
2. ROGERS, S.E., *Progress in high-lift aerodynamic calculations*, AIAA Paper **93-0194**, 1993.
3. VALEREZO, W.O., MAVRIPLIS, D.J., *Navier-Stokes applications to high-lift airfoil analysis*, AIAA Paper **93-3534**, 1993.
4. CEBECI, T., *Calculation of multielement airfoils and wings at high lift*, AGARD Conference Proceedings 515 on high-lift aerodynamics, Paper **24**, Alberta, Canada, Oct. 1992.
5. CEBECI, T., BESNARD, E., MESSIE, S., *A stability transition-interactive-boundary-layer approach to multielement wings at high lift*, AIAA Paper **94-0292**, 1994.
6. NIELD, N.B., *An overview of the 777 high lift aerodynamic design*, Proceedings of High Lift and Separation Control Conference, Royal Aeronautical Society, March 1995.
7. JAMESON, A., *Acceleration of transonic potential flow calculation on arbitrary meshes by the multiple grid method*, AIAA Paper **79-1458**, 1979.
8. DUMITRESCU, H., CARDO, V., *New boundary layer equations*, Proceedings of the Romanian Academy, Series A, 2, 1-2, 2001.
9. CEBECI, T., *An engineering approach to the calculation of aerodynamic flows*, Springer Verlag, 2000.
10. FIDLER, H., HEAD, M.R., *Intermittence measurements in the turbulent boundary layer*, Journal of Fluid Mechanics, **25**, Part 4, 1966.
11. ABBOTT, I.H., VON DOENHOFF, A.E., *Theory of wing sections*, Dover Publications Inc., New York, 1959.
12. COUSTEIX, J., PAILHAS, G., *Étude exploratoire d'un processus de transition laminaire-turbulent au voisinage de d'écoulement d'une couche limite laminaire*, La Recherche Aérospatiale, **3**, 1979.

Received January 28, 2002
